Submitted to Nuovo Cimento

CERN/TC/PHYSICS 64-2
3rd February, 1964

On the Associated Production of K - Y Pairs by 10 GeV/c π^- in the Hydrogen Bubble Chamber

A. Bigi*, S. Brandt, W.A. Cooper, Aurelia de Marco,** Ch. Peyrou
R. Sosnowski,*** A. Wróblewski****

CERN

Geneva

1. INTRODUCTION

The production of strange particles in π^- proton interactions at high energy ($p_{\pi^-} \gtrsim 5$ GeV/c) has been first studied in bubble chamber experiments at Dubna[1] and at CERN[2]. These experiments have demonstrated that Λ^0 hyperons, and to a lesser extent Σ hyperons, show a pronounced backward peaking in the cm system of π^--p; that the K^0 mesons are significantly peaked forward, and that the mechanism of production is therefore a "peripheral" rather than a statistical one. However, these studies were based essentially on events with only one strange particle decay visible in the chamber, so that the $K\bar{K}$ events could not be separated from the YK events and it was not possible to draw any more detailed conclusion about the mechanism of different channels of strange particle production.

In order to get more detailed information about the associated production of strange particles, in 1961 an exposure of the 81 cm Saclay hydrogen bubble chamber to a 10 GeV/c π^- beam was carried out and only those photographs studied that showed a π^--p interaction together with the decay of two strange particles in the chamber. Preliminary results were presented at the 1962 Conference on High Energy Physics at CERN[3].

---

* University of Pisa, Italy

** Now at the University of Torino, Italy

*** On leave from the Institute for Nuclear Research, Warsaw, Poland

**** On leave from the Institute of Experimental Physics, University of Warsaw, Poland

PS/4195/dac

At that conference the results of two other "2V" experiments - performed with heavy liquid bubble chambers - were presented[4][5]. The Dubna group[4] has studied a sample of 52 $\Lambda^o K^o$ and 37 $K^o\bar{K}^o$ events produced by 7 GeV/c π^-. The CERN-Paris group[5] has studied $K^o\Lambda^o$ and $K^o\bar{K}^o$ production by π^- at 6, 11 and 18 GeV/c. Two more papers on the production of strange particles by high energy π^- in hydrogen were published later. Bertanza et al.[6] have studied the problem at 4.7 GeV/c and Ferbel and Taft[7] at 11 GeV/c.

This paper contains our results on KY production by 10 GeV/c π^- in hydrogen. The analysis of $K\bar{K}$ production is presented in a separate paper[8].

2. EXPERIMENTAL PROCEDURE

The exposure of the 81 cm Saclay hydrogen bubble chamber to a high energy π^- beam from the CERN proton synchrotron yielded about 83000 photographs with an average of 10.5 beam tracks per picture. The beam momentum was measured to be (10.0 ± 0.6) GeV/c. The contamination of μ^- and K^- were estimated to be $\sim$14 o/o and $<$ 1 o/o respectively.

All photographs were scanned twice for V^o and V^+ decays associated with a beam interaction in a fiducial region of the chamber. Several thousand decays were found, among them 325 events with both V's decaying in the chamber. The efficiency of scanning was calculated separately for different types of V decay (see Appendix).

All events with 2 V's were measured using the CERN Iep measuring machines. Geometrical reconstruction and kinematical fitting of V's was done on an IBM 709 computer using the GAP programme[9]. Using the χ^2 value for testing the goodness of different fits it was in most cases possible to identify the V's. In ambiguous cases (K^o or Λ^o, Σ^+ or K^+) ionisation measurements using the mean gap length method[10] were carried out.

Kinematic quantities that are not given by the GAP programme such as cms momenta and angles, Q - values for pairs and triplets of secondary particles etc. were computed by a special analysis programme (SAP)[11] on the IBM 709 computer.

For the final analysis events with a distance < 20 cm from the far end of the chamber were omitted in order to have no events with a big weight for escape probability. The resulting average weight of events (excluding events with a charged kaon) was 1.45.

3. EXPERIMENTAL RESULTS

3.1 Cross Sections

The total number of events observed and corrected in each K - Y production channel is given in Table I.

Table I

Event type	Number observed	Number$^{\Phi}$ corrected	σ(mb)$^{\Phi\Phi}$
$\pi^- + p \rightarrow \Lambda^o(\Sigma^o) + K^o + n\pi$	95	595 ± 61	0.472 ± 0.048
$\Lambda^o(\Sigma^o) + K^+ + n\pi$	11	539 ± 162	0.422 ± 0.127
$\Sigma^+ + K^o + n\pi$	32	124 ± 22	0.097 ± 0.017
$\Sigma^+ + K^+ + n\pi$	5	118 ± 53	0.092 ± 0.041
$\Sigma^- + K^o + n\pi$	43	202 ± 31	0.158 ± 0.024
$\Sigma^- + K^+ + n\pi$	13	206 ± 66	0.161 ± 0.052
$\Xi^- + 2K + n\pi$	12	19.8 ± 5.7	0.0155 ± 0.0045
$Y + \bar{Y} + N + n\pi$	3	8.1 ± 4.6	0.0063 ± 0.0036

$^{\Phi}$ To calculate the correction we made use of:

a) the known values of life-time for strange particles (W.H. Barkas, A.H. Rosenfeld, UCRL 8030 (1960))

b) the value of the branching ratio $\frac{K^o \rightarrow 2\pi}{K^o \rightarrow \text{all modes}} = 0.335 \pm 0.014$ (J.L. Brown et al., Phys. Rev. 130, 769)

c) the assumption that the value of branching ratio is $K_1^o / K_2^o = 1$

d) the branching ratio $\frac{\Lambda^o \rightarrow \pi^o + n}{\Lambda^o \rightarrow \text{all modes}} = 1/3$

e) scanning efficiency for V^o and $V^{\pm}$, as calculated in the Appendix

$^{\Phi\Phi}$ To normalise our data the total cross section $\sigma^{tot}_{\pi^- p} = (26.5 \pm 0.5)$ mb at this momentum was used (von Dardel et al., Phys. Rev. Letters 8, 173 (1962)

It can be seen that the values listed in Table I are not in disagreement with the assumption that for a given K - Y pair every possible combination of charge has the same probability, that is:

$$N_{\Lambda^0(\Sigma^0)K^0} = N_{\Lambda^0(\Sigma^0)K^+}\ ,\ N_{\Sigma^-K^0} = N_{\Sigma^-K^+}\ ,\ N_{\Sigma^+K^0} = N_{\Sigma^+K^+}$$

though the statistics of the K^+ channels are too small to prove these equalities. Nevertheless, assuming these equalities to be true, we find

$$\sigma(\pi^- p \to \Lambda^0 K) = 2\sigma(\pi^- p \to \Lambda^0(\Sigma^0)K^0) = (0.94 \pm 0.10)\ \text{mb}$$

$$\sigma(\pi^- p \to \Sigma^\pm K) = 2\sigma(\pi^- p \to \Sigma^\pm K^0) = (0.51 \pm 0.07)\ \text{mb}$$

The total observed cross section $\sigma(\pi^- p \to YK) = (1.45 \pm 0.17)$ mb is compared in Table II with the results obtained in other experiments.

Table II

Cross sections for $\pi^- + p \to Y + K + n\pi$

Momentum GeV/c	$\sigma(\pi^- p \to Y^0 K)$ mb	$\sigma(\pi^- p \to YK)$ mb	Laboratory and reference
4.7	0.80	1.11	Brookhaven[6]
7 - 8	0.80 ± 0.25	-	Dubna[1]
10	0.94 ± 0.10	1.45 ± 0.17	CERN - this experiment
16	0.68 ± 0.10	1.32 ± 0.15	CERN[2]

Though no fit was performed to the interaction point the missing mass, energy and momentum as calculated in SAP allowed to establish the number of produced neutral pions to be 0, 1 or ≥ 2. The classification of $Y - K^0$ events according to the number and charge of produced pions is given in Table III. It should be remembered, however, that this classification is for π^0's rather statistical and not based on absolute certainty for each individual event.

Table III

Event type	Number of events observed	Number of events corrected for escape probability	σ mb
$\pi^- + p \rightarrow \Lambda^0 + K^0$	3	7.29	0.026
$\Lambda^0 + K^0 + \pi^0$	2	3.18	0.011
$\Lambda^0 + K^0 + \geqslant 2\pi^0$	11	19.95	0.072
$\Lambda^0 + K^0 + \pi^+ + \pi^-$	8	9.54	0.034
$\Lambda^0 + K^0 + \pi^+ + \pi^- + \pi^0$	12	14.82	0.053
$\Lambda^0 + K^0 + \pi^+ + \pi^- + \geqslant 2\pi^0$	26	35.83	0.129
$\Lambda^0 + K^0 + 2\pi^+ + 2\pi^-$	2	2.21	0.008
$\Lambda^0 + K^0 + 2\pi^+ + 2\pi^- + \pi^0$	15	18.07	0.065
$\Lambda^0 + K^0 + 2\pi^+ + 2\pi^- + \geqslant 2\pi^0$	14	17.62	0.063
$\Lambda^0 + K^0 + 3\pi^+ + 3\pi^-$	0	0	-
$\Lambda^0 + K^0 + 3\pi^+ + 3\pi^- + \pi^0$	1	1.45	0.005
$\Lambda^0 + K^0 + 3\pi^+ + 3\pi^- + \geqslant 2\pi^0$	1	1.39	0.005
Total $\pi^- + p \rightarrow \Lambda^0 + K^0 +$ pions	95	141.35	0.472
$\pi^- + p \rightarrow \Sigma^- + K^0 + \pi^-$	2	3.69	0.009
$\Sigma^- + K^0 + \pi^- + \pi^0$	7	15.36	0.036
$\Sigma^- + K^0 + \pi^- + \geqslant 2\pi^0$	10	13.51	0.032
$\Sigma^- + K^0 + 2\pi^- + \pi^+$	2	3.68	0.009
$\Sigma^- + K^0 + 2\pi^- + \pi^+ + \pi^0$	9	12.11	0.029
$\Sigma^- + K^0 + 2\pi^- + \pi^+ + \geqslant 2\pi^0$	8	9.29	0.022
$\Sigma^- + K^0 + 3\pi^- + 2\pi^+$	0	0	-
$\Sigma^- + K^0 + 3\pi^- + 2\pi^+ + \pi^0$	2	2.65	0.006
$\Sigma^- + K^0 + 3\pi^- + 2\pi^+ + \geqslant 2\pi^0$	3	6.27	0.015
Total $\pi^- + p \rightarrow \Sigma^- + K^0 +$ pions	43	66.56	0.158

$\pi^- + p \rightarrow \Sigma^+ + K^o + \pi^-$	0	0	-
$\Sigma^+ + K^o + \pi^- + \pi^o$	5	6.62	0.016
$\Sigma^+ + K^o + \pi^- + \geqslant 2\pi^o$	8	10.23	0.024
$\Sigma^+ + K^o + 2\pi^- + \pi^+$	2	2.06	0.005
$\Sigma^+ + K^o + 2\pi^- + \pi^+ + \pi^o$	10	12.90	0.031
$\Sigma^+ + K^o + 2\pi^- + \pi^+ + \geqslant 2\pi^o$	3	3.60	0.008
$\Sigma^+ + K^o + 3\pi^- + 2\pi^+$	0	0	-
$\Sigma^+ + K^o + 3\pi^- + 2\pi^+ + \pi^o$	3	4.19	0.010
$\Sigma^+ + K^o + 3\pi^- + 2\pi^+ + \geqslant 2\pi^o$	1	1.23	0.003
Total $\pi^- + p \rightarrow \Sigma^+ + K^o +$ pions	32	40.83	0.097

3.2 CM System distributions

The further analysis of the Y - K production is based on $\Lambda^o K^o$, $\Sigma^+ K^o$ and $\Sigma^- K^o$ events.

a) $\Lambda^o K^o$ events

We shall call these events $\Lambda^o K^o$ events though a large number of them may in fact be $\Sigma^o K^o$ events.

In Fig. 1 the $p_\perp - p_L^*$ plot with its different projections gives information on the Λ^o distribution in the cm system of $\pi^- p$. There is a remarkable resemblance between the presented distributions and those for protons from the reactions of $K^o K^o$ production[8]. The main characteristic features of Λ^o emission are as follows:

1. Limited transverse momenta which are much lower than allowed by phase space.

2. Strong backward-forward asymmetry. Fifty percent of Λ^o hyperons are emitted with $\cos \theta^*$ less than -0.9 and the average longitudinal cm momentum of Λ^o is -0.70 GeV/c. The lack of the fast forward Λ^o-hyperons is statistically significant and cannot be due to experimental bias. The backward-forward ratio corrected for detection probability is $B/F = 4.3 \pm 1.1$.

The cms distributions for K^o mesons are presented in the same form as for Λ^o hyperons in Fig. 2. It can be seen that:

1. The transverse momenta are limited to low values.

2. K^o mesons are emitted predominantly forward. The average longitudinal cms momentum equals + 0.27 GeV/c.

As already discussed[3], there exists a strong correlation between Λ^o and K^o from the same interaction. In about 70 o/o of the events these particles are emitted into opposite hemispheres. If one tries to describe the interaction in terms of the one particle exchange model, the process of $\Lambda^o K^o$ production would be described rather as a strangeness carrying particle exchange and

not as an exchange of a particle with strangeness zero[φ].

The pions (Fig. 3) have still smaller transverse momenta and a nearly symmetric distribution in p_L^*. Most of them have low values of p_L^*, in 65 o/o of cases below 0.5 GeV/c.

b) Σ^+K^o events

The Σ^+ hyperons (Fig. 4) give a corrected backward-forward ratio of $B/F = 5.0 \pm 2.4$, the average p_L^* is -0.61 GeV/c. Contrary to what was observed in Λ^oK^o events there exist some fast forward hyperons.

The emission of kaons (Fig. 5) and pions (Fig. 6) show the same main features as in Λ^oK^o events. In particular, the same strong angular correlation of a kaon and a hyperon from the same event is also observed.

c) Σ^-K^o events

The emission of Σ^- hyperons (Fig. 7) is quite different from the general trend of baryons to have the same cms direction as the proton before the collision. The distribution in p_L^* is almost symmetric about $p_L^* = 0$, as can be seen from the average of p_L^* which is equal to -0.22 GeV/c. The backward-forward ratio $B/F = 1.7 \pm 0.5$.

For both Σ^+ and Σ^- the p_L^* distribution extends to larger positive values of p_L^* than for Λ.

The distributions for K^o mesons and pions produced together with Σ^- hyperons are shown in Fig. 8 and Fig. 9 respectively.

d) Ξ^- events

Eleven out of 12 observed Ξ^- hyperons are emitted in the backward hemisphere. The average cms longitudinal momentum equals -0.68 GeV/c.

φ Indeed, in any mechanism of π exchange (or generally no strangeness carrying meson exchange) Λ and K will be emitted at the same vertex and therefore go together in spite of the fact that the phase space favours the emission of the two heaviest particles produced in the opposite directions.

3.3 Invariant mass distributions

The distributions of the invariant mass for all two and three particle combinations were studied. The "background" was not calculated according to the normal phase space formulae as it seems to have little meaning for high energy interactions because of their strong non-statistical nature. The results on the production of bound states have therefore a qualitative character.

The invariant mass distribution of $K^{o}\pi^{+}$ system compared to a "background" distribution of $K^{o}\pi^{-}$, which cannot carry a positive strangeness (Fig. 10, b, c) indicates clearly that a K^{*}_{888} is produced. This comparison gives, however, only a lower limit of K^{*} production because we were plotting for each event all possible $K^{o}\pi^{+}$ combinations and therefore besides the "true" combinations there is a large background of "spurious" combinations. The upper limit for K^{*} production can be obtained from the "enhanced" distribution (Fig. 10, a) in which all other combinations of $K^{o}\pi^{+}$ were erased if in a given event one combination corresponding to a K^{*} mass 888 $\pm$ 50 MeV was found. We conclude that in the Y - K^{o} events the positive K^{*} is produced in 10 o/o to 25 o/o of the events.

The invariant mass distribution of $\Lambda^{o}\pi^{+}$ and $\Lambda^{o}\pi^{-}$ combinations (Fig. 11) shows a small peak near the position of Y^{*}_{1385}. In the distribution of $\Sigma^{+}\pi^{-}$ and $\bar{\Sigma}^{-}\pi^{+}$ mass combinations (Fig. 12) there is an indication of production of Y^{*}_{1405} and Y^{*}_{1520}. The statistics of Ξ^{-} events is too small to draw any definite conclusions but it is interesting to notice that half of the $\Xi^{-}\pi^{-}$ combinations have the mass close to the Y^{*}_{1535}.

3.4 Multiplicity of pions

The number of neutral pions produced per interaction as estimated from the missing mass, energy and momentum is slightly higher than the value 1/2 $n_{\pi^{\pm}}$ expected from charge symmetry. This is shown in Table IV where the total expected average multiplicity of pions 3/2 $n_{\pi^{\pm}}$ is compared with the observed one $n_{\pi^{\pm}} + n_{\pi^{o}}$. The latter value represents in fact a lower limit for the number of pions because we are not able to estimate correctly the number of neutral pions if it is greater than 1 and all such events were taken as containing $2\pi^{o}$.

Table IV

Multiplicity of charged and neutral pions

$p_L^*(\Lambda^o)$ interval	$3/2\, n_{\pi^\pm}$	$n_{\pi^\pm}+n_{\pi^o}$	Number of events
$-1.8 \div -1.3$	1.1	$\geqslant 2.6$	17
$-1.3 \div -0.9$	2.0	$\geqslant 3.0$	16
$-0.9 \div -0.5$	3.4	$\geqslant 4.0$	20
$-0.5 \div 0.0$	4.7	$\geqslant 4.6$	21
$0.0 \div +0.4$	5.4	$\geqslant 5.4$	9
$+0.4 \div +0.8$	4.4	$\geqslant 4.6$	9
All $\pi^- + p \rightarrow K^o + \Lambda^o +$ pions	3.49	$\geqslant 3.84$	92$^\Phi$
All $\pi^- + p \rightarrow K^o + \Sigma^- +$ pions	3.43	$\geqslant 3.62$	43
All $\pi^- + p \rightarrow K^o + \Sigma^+ +$ pions	3.66	$\geqslant 3.76$	32

Table V

$p_\perp$ - mass dependence

Particle	Average $p_\perp$
π^o	0.30 ± 0.02 GeV/c
$\pi^\pm$	0.32 ± 0.01 "
K^o	0.37 ± 0.02 "
Λ^o	0.47 ± 0.02 "
$\Sigma^\pm$	0.53 ± 0.03 "
Ξ^-	0.58 ± 0.06 "

$^\Phi$ Three events which are very probably pure associated production $\pi^- + p \rightarrow K^o + \Lambda^o$ have been omitted

PS/4195/dac

The $K^{o}\Lambda^{o}$ events for which the statistics were largest were divided into six groups according to the longitudinal cms momentum of Λ^{o} hyperon. It can be seen from Table IV that the excess of the number of π^{o} measons occurs mainly in the events with fast backward Λ^{o}. In other words, the correlation between the multiplicity of pions and the change of energy of the baryon in cms exists but is less pronounced than one would have thought in looking at charged pions only.

It could be thought that for events with a low multiplicity of charged pions the errors on the missing mass are larger than for fast jets with large multiplicity. This is not so, because for the fast type of jets the Λ^{o} is slow in the lab system and therefore measured accurately so that the errors in missing mass calculation are practically the same for all types of jets. Hence, the effect found on the multiplicity of π^{o}'s does not seem to correspond to a bias due to the uncertainty in the missing mass calculation.

3.5 Transverse momentum $p_{\perp}$ and total cms momentum p^{*}

At the 1962 CERN Conference it was shown[3] that the average transverse momentum increases with the mass of the produced particle. This fact was confirmed later in other experiments[7][12]. The present data based on greater statistics (Table V) confirms the previous result and makes the $\bar{p}_{\perp}$ mass dependence even more significant. Fig. 13 shows the $p_{\perp}$ distributions for different particles. The histograms are normalised to equal area. The average value of $p_{\perp}$ for π^{o} measons was calculated on the basis of missing $p_{\perp}$ in 66 events (see Table III) for which the missing mass, energy and momentum calculations indicate the production of $1\pi^{o}$. This is justified because the large spread of the beam momentum (10.0 ± 0.6 GeV/c) influences strongly the longitudinal component of π^{o} momentum but does not change the value of the transverse momentum.

We find that there is a difference in $\bar{p}_{\perp}$ between Λ^{o}'s emitted strongly backwards in the cms and the less "peripheral" Λ^{o}'s (see Table VI). A similar and even more significant $\bar{p}_{\perp} - p_{L}^{*}$ dependence was found in the case of protons emitted in the $K\bar{K}$ producing reactions[12].

It should be noted that this effect is not a reflection of momentum conservation as can be seen in Fig. 1.

Table VI

Interval of $p_L^*(\Lambda^o)$	Average $p_\perp$	Number of events$^\Phi$
-1.8 ÷ -1.3 GeV/c	0.37 ± 0.04 GeV/c	17
-1.3 ÷ -0.5 "	0.47 ± 0.04 "	36
-0.5 ÷ +0.8 "	0.51 ± 0.04 "	39

The transverse momentum - mass dependence is probably a reflection of a much stronger dependence of total cms momentum on mass. The $\bar{p}^*$ mass dependence is shown in Table VII.

For all of the investigated reactions the $\bar{p}^*$-m dependence can be well approximated by a linear function:

$$\bar{p}^* = am + b$$

It seems that the "slope" a is almost the same for all the reactions (see Table VII). At these energies the statistical theory also predicts some $\bar{p}^*$ mass dependence but the slope a equals only about 0.30 instead of 0.52 observed. A $\bar{p}^*$ - m dependence as strong as that observed could be obtained if the observed particles were produced via certain intermediate states. The present experiment shows however, that none of the known resonances dominates the production of secondaries. The same was shown to be true for $K\bar{K}$ producing reactions[8][12]. It is interesting to notice that even assuming a 100 o/o production of known resonances one gets a $\bar{p}^*$ - m dependence weaker than the experimental one if the momentum spectrum of those bound states is calculated according to phase-space.

3.6 Y - $\bar{Y}$ events

It is impossible to draw any conclusion about Y - $\bar{Y}$ production

---

$^\Phi$ Three events which very probably represent pure associated production $\pi^- + p \rightarrow K^o + \Lambda^o$ have not been taken into account

on the basis of three events. It is interesting to notice, however, that two events are of the type: $\pi^- + p \rightarrow \Lambda^o + \bar{\Lambda}^o + \pi^+ + \pi^- + n$, with both Λ^o and $\bar{\Lambda}^o$ emitted backwards with small p^*. The third event is of the type: $\pi^- + p \rightarrow \bar{\Lambda}^o + \Sigma^+ + \pi^- + n$, Σ^+ is emitted backwards, Λ^o forward and p^* is also small.

Table VII

Average $\bar{p}^{*}$ (GeV/c)

Reaction	Particle						"Slope" a of $\bar{p}^{*}=am+b$ dependence
	π^+	K^o	Λ^o	Σ^+	Σ^-	Ξ^-	
$\pi^-+p \rightarrow \Lambda^o+K^o+n\pi$	$0.47^{-0.01}_{+0.03}$	$0.68^{-0.03}_{+0.08}$	$0.98^{-0.03}_{+0.07}$	-	-	-	0.53 ± 0.05
$\pi^-+p \rightarrow \Sigma^++K^o+n\pi$	$0.50^{-0.03}_{+0.02}$	$0.70^{-0.06}_{+0.06}$	-	$1.06^{-0.09}_{+0.07}$	-	-	0.54 ± 0.07
$\pi^-+p \rightarrow \Sigma^-+K^{\bullet}+n\pi$	$0.49^{-0.03}_{+0.05}$	$0.76^{-0.06}_{+0.13}$	-	-	$0.99^{-0.07}_{+0.10}$	-	0.49 ± 0.09
$\pi^-+p \rightarrow \Xi^-+2K+n\pi$ [⊕]	0.39 (23)	0.59 (17) [⊕⊕]	-	-		0.94 (12)	~ 0.48

[⊕] For this reaction the statistics were insufficient to calculate reasonable errors. Instead, the number of particles is given in brackets after the values for $\bar{p}^{*}$

[⊕⊕] Including few K^+

PS/4195/dac

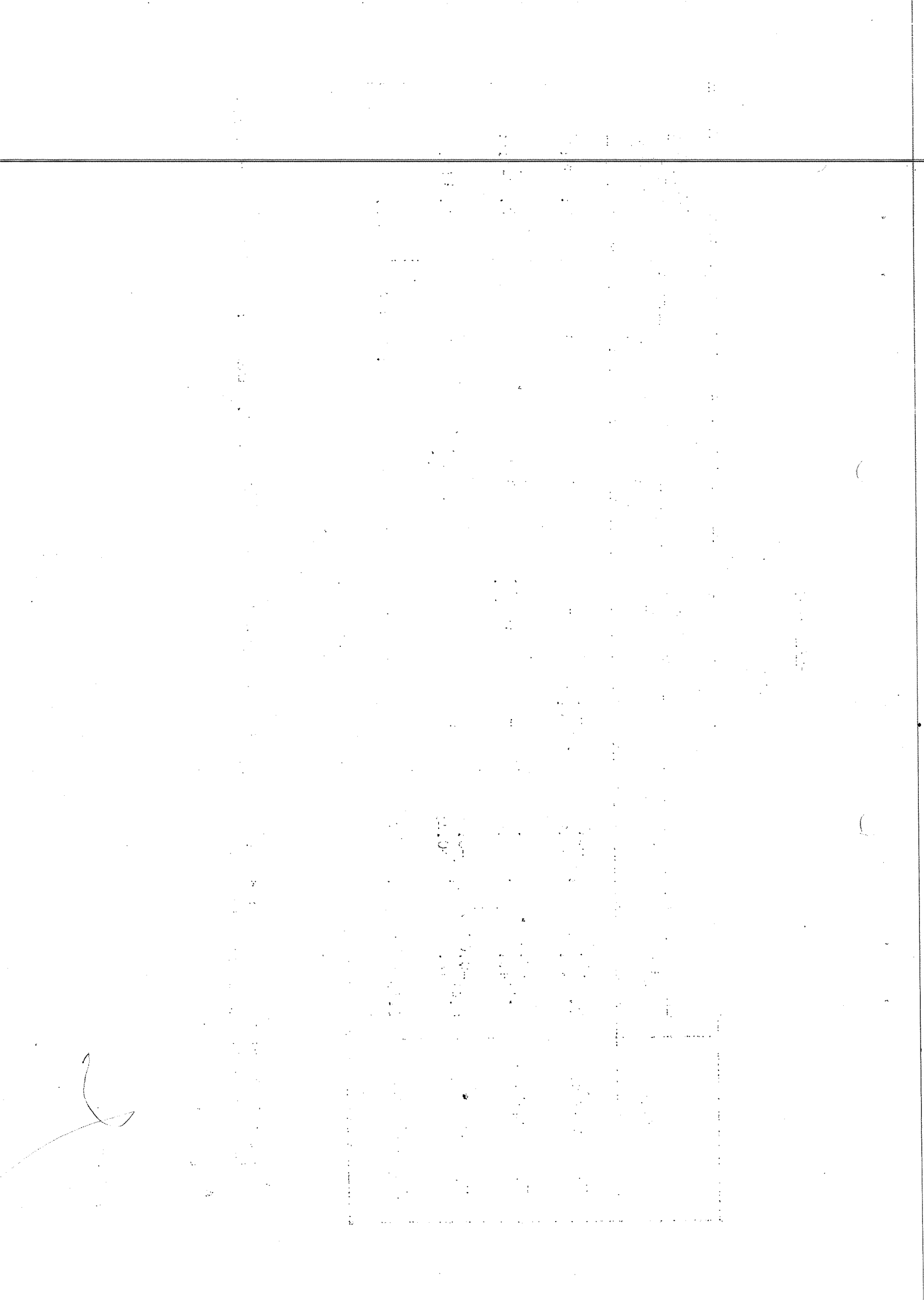

4. CONCLUSIONS

4.1 Emission of baryons

As was already found [1][2] Λ^o hyperons produced in the collisions at energies discussed are emitted predominantly in the backward hemisphere. The comparison of the cms distribution of Λ^o hyperons with those of nucleons [8][12][13] shows that there is a remarkable resemblance between Λ^o and nucleon emission.

The Σ^+ hyperons are not so well collimated in the backward direction. We mean by this that there are some events with a forward emission of fast Σ^+. In addition, the average transverse momentum is somewhat higher for Σ^+ than for Λ^o. It is interesting to notice that the distribution of Σ^+ produced in high energy p - p collisions shows even more clearly the deviation from the distribution of Λ^o from the same collisions [14].

The Σ^- hyperons are much less peaked backward in the cms of π^--p. There is nearly no backward-forward asymmetry. Comparison of Σ^- and Λ^o production shows that the mechanism of collision with Σ^- emission is different from that with Λ^o and nucleon emission.

For experimental reasons (identification of baryons) it is often much easier to study hyperon emission than the emission of nucleons. According to the present results the sample of Λ^o could be representative for the collisions with nucleon emission, as was found by studying the reactions with $K^o\bar{K}^o$ produced [8][12] and collisions with 5 pions produced [13]. The reactions with Σ^- hyperons are not representative for the no strangeness producing collisions.

4.2 Bound states

At lower energies the inelastic collisions of elementary particles are dominated by the production of bound states (resonances). This seems not to be the case at energies as high as 10 GeV where we find that bound states such as K^*_{888}, Y^*_{1385}, Y^*_{1405}, Y^*_{1520} are produced in several percent of the interactions only. A similar result was obtained in a study of $K\bar{K}$ producing reactions [8][12].

4.3 p^{*} - m and $p_{\perp}$ - m dependence

It was found that both the average total cms momentum and the average transverse momentum of secondary particles depend strongly on their mass. It is possible that this characteristic feature of strange particle production in π^--p collisions at high energy can be well explained assuming the existence of at least two "intermediate states": $\pi^- + p \rightarrow A+B$. Here A and B may represent in certain cases known isobars, but generally other states which subsequently "decay" into the "final" secondary particles: pions, kaons and baryons or known isobars.

A more detailed kinematic analysis of our events in terms of this model is being made.

ACKNOWLEDGEMENTS

We would like to thank the CERN Track Chambers Division and especially Drs. J. Bartke, A. Cooper and H. Filthuth for the construction of the high energy pion beam and for helping during the taking of photographs. Our thanks are due to Prof. B. Gregory and the crew of the Ecole Polytechnique 81 cm hydrogen bubble chamber for providing and operating the chamber. Drs. J. Bartke, R. Carrara, B. Czapp and G.R. Macleod helped to scan the photographs in the first stages of this experiment. We have to thank the Iep group of CERN for their careful measurements and Mme F. Delerce and Mlle R. Tzschernig for their constant help in preparation of measurements, plotting of results and carrying out various calculations.

We are grateful to Dr. H.H. Bingham and Dr. D.R.O. Morrison for many stimulating and fruitful discussions.

APPENDIX

The statistics of "V" and "2V" events found in a double scanning were studied carefully in order to estimate the efficiency of finding different types of decay. For all two-body hyperon and kaon decays we have constructed a p_{Lab} - cos θ^{**} plot, p_{Lab} being the laboratory momentum of the decaying particle, θ^{**} being the angle of emission of the secondary particle in the cm system of the decaying particle. On this diagram we have plotted the curves of constant laboratory angle of decay (opening angle for V^o particles), and constant laboratory momentum of secondary particles from the decay. If there is no forward-backward asymmetry of emission of secondaries in the cms of the decaying particle, there should be a uniform distribution of events along the cos θ^{**} axis for all the sample as well as for a chosen interval of p_{Lab}. One can therefore study scanning biases for decays with given laboratory characteristics.

Figs. 14, 15 and 16 represent p_{Lab} - cos θ^{**} plots for the decays:

$$\Lambda^o \longrightarrow p + \pi^-, \quad \Sigma^+ \longrightarrow p + \pi^o \text{ and } \Sigma^+ \longrightarrow \pi^+ + n$$

Considering Λ^o decay one can expect lower scanning efficiency for "V^o" with a small opening angle ($\theta < 5^o$) and for decays with very short pion track ($p_\pi < 50$ MeV/c). However, plotting Λ^o events found in scanning on a plot (Fig.13) no deficiency of points in any part of the plot was found within the statistical uncertainty. We consider therefore that Λ^o events were found in scanning with a constant scanning efficiency equal to about 99 o/o.

The same efficiency applies for K^o events.

For $V^{\pm}$ decays the efficiency of scanning depends strongly on the laboratory angle of decay. The dependence shown in Fig. 17 was calculated taking the number of events with a given angle of decay which were found in both scannings and found only once. Integrating plots shown in Figs. 15 and 16 over the laboratory angles which occur for a Σ decay with given laboratory momentum we have obtained the efficiency of scanning for Σ decay as a function of Σ laboratory momentum (Fig. 18). This correction was then applied to account for scanning loss of Σ_π and Σ_p decays.

FIGURE CAPTIONS

Fig. 1 $p_\perp - p_L^*$ plot for Λ^o's from the reaction $\pi^- + p \to K^o + \Lambda^o$ + pions. Histograms are given for p_L^*, p^*, $p_\perp$ and cos θ^*. Broken lines give uncorrected number of events. Solid lines include corrections for detection probability

Fig. 2 $p_\perp - p_L^*$ plot for K^o's from the reaction $\pi^- + p \to K^o + \Lambda^o$ + pions

Fig. 3 $p_\perp - p_L^*$ plot for charged pions from the reaction $\pi^- + p \to K^o + \Lambda^o$ + pions

Fig. 4 $p_\perp - p_L^*$ plot for Σ^+'s from the reaction $\pi^- + p \to K^o + \Sigma^+$ + pions

Fig. 5 $p_\perp - p_L^*$ plot for K^o's from the reaction $\pi^- + p \to K^o + \Sigma^+$ + pions

Fig. 6 $p_\perp - p_L^*$ plot for charged pions from the reaction $\pi^- + p \to K^o + \Sigma^+$ + pions

Fig. 7 $p_\perp - p_L^*$ plot for Σ^-'s from the reaction $\pi^- + p \to K^o + \Sigma^-$ + pions

Fig. 8 $p_\perp - p_L^*$ plot for K^o's from the reaction $\pi^- + p \to K^o + \Sigma^-$ + pions

Fig. 9 $p_\perp - p_L^*$ plot for charged pions from the reaction $\pi^- + p \to K^o + \Sigma^-$ + pions

Fig. 10 Q-value spectrum of $(K^o\pi^+)$-system (B) and $(K^o\pi^-)$-system (C). The latter serves as a background. (A) gives the enhanced Q-value spectrum of the $(K^o\pi^+)$-system (see text).

Fig. 11 Combined Q-value spectrum of $(\Lambda^o\pi^+)$ and $(\Lambda^o\pi^-)$-systems

Fig. 12 Combined Q-value spectrum of $(\Sigma^-\pi^+)$ and $(\Sigma^+\pi^-)$-systems

Fig. 13 $p_\perp$ distributions for different particles. Histograms are normalised to equal area

Fig. 14 p_{Lab} - cos θ^{**} plot for the decay $\Lambda^o \to p + \pi^-$. Lines of constant lab. angle of pion (solid), lab. momen. of proton (dashed) and lab. momen. of pion (dash-dotted) are given

Fig. 15 p_{Lab} - cos θ^{**} plot for the decay $\Sigma^+ \to p + \pi^o$ (dash-dotted) are given. Lines represent constant lab angle (solid) and lab. momentum (dashed) of proton

Fig. 16 p_{Lab} - cos θ^{**} plot for the decay $\Sigma^+ \to n + \pi^+$. Lines represent constant lab. angle (solid) and Lab. momentum (dashed) of pion

Fig. 17 Dependence of the scanning efficiency for Σ's on the lab. angle of decay

Fig. 18 Dependence of the scanning efficiency for Σ's on the Σ lab. momentum

PS/4195/dac

REFERENCES

1. M.I. Soloviev, Proceedings of the 1960 International Conference on High Energy Physics at Rochester, p. 388

2. J. Bartke, R. Budde, W.A. Cooper, H. Filthuth, Y. Goldschmidt-Clermont, G.R. Macleod, A. de Marco, A. Minguzzi-Ranzi, L. Montanet, D.R.O. Morrison, S. Nilsson, Ch. Peyrou, R. Sosnowski, A. Bigi, R. Carrara, C. Franzinetti, I. Manelli, G. Brauti, M. Ceschia, L. Chersovani - ibid., p. 402 and Nuovo Cimento 24, 876 (1962)

3. A. Bigi, S. Brandt, R. Carrara, W.A. Cooper, A. de Marco, G.R. Macleod, Ch. Peyrou, R. Sosnowski, A. Wroblewski - Proceedings of the 1962 International Conference on High Energy Physics at CERN, p. 247

4. V.A. Belyakov, Wang Yung-Chang, V.I. Veksler, N.M. Viryasov, Du Yuan-cai, Kim Hi In, E.N. Kladnitskaya, A.A. Kuznetsov, A. Mikhul, Nguyen Dinh-Tu, V.N. Penev, E.S. Sokolova, M.I. Soloviev - ibid., p. 261 and p. 336

5. H.H. Bingham, M. Bloch, D. Drijard, A. Minguzzi-Ranzi, M. Nicolić - ibid., p. 240 (see also Nuovo Cimento 29, 339 (1963))

6. L. Bertanza, B.B. Culwick, K.W. Lai, I.S. Mitra, N.P. Samios, A.M. Thorndike, S.S. Yamamoto, R.M. Lea, Phys. Rev. 130, 786 (1963)

7. T. Ferbel, H. Taft, Nuovo Cimento 28, 1214 (1963)

8. A. Bigi, S. Brandt, W.A. Cooper, A. de Marco, Ch. Peyrou, R. Sosnowski, A. Wroblewski - Nuovo Cimento, to be published

9. A. Kernan, R. Böck, W.G. Moorhead - Internal CERN/DD report (1961)

10. C. Dilworth, D.R.O. Morrison, G. Membriani - Nuovo Cimento - to be published

11. S. Brandt - CERN Internal Note DD/EXP/62/25 and S. Brandt - Dissertation, Bonn University (1963)

12. S. Brandt, A. Wroblewski - Proceedings of the 1963 International Conference on Elementary Particles in Sienna

13. M. Bardadin, L. Michejda, S. Otwinowski, R. Sosnowski - ibid.

14. J. Bartke, W.A. Cooper, B. Czapp, H. Filthuth, Y. Goldschmidt-Clermont, L. Montanet, D.R.O. Morrison, S. Nilsson, Ch. Peyrou, R. Sosnowski, A. Bigi, R. Carrara, C. Franzinetti, P. Manelli, Nuovo Cimento 29, 8 (1963)

PS/4195/dac

$P_\perp - P_L^*$ PLOT FOR Λ° PRODUCTION

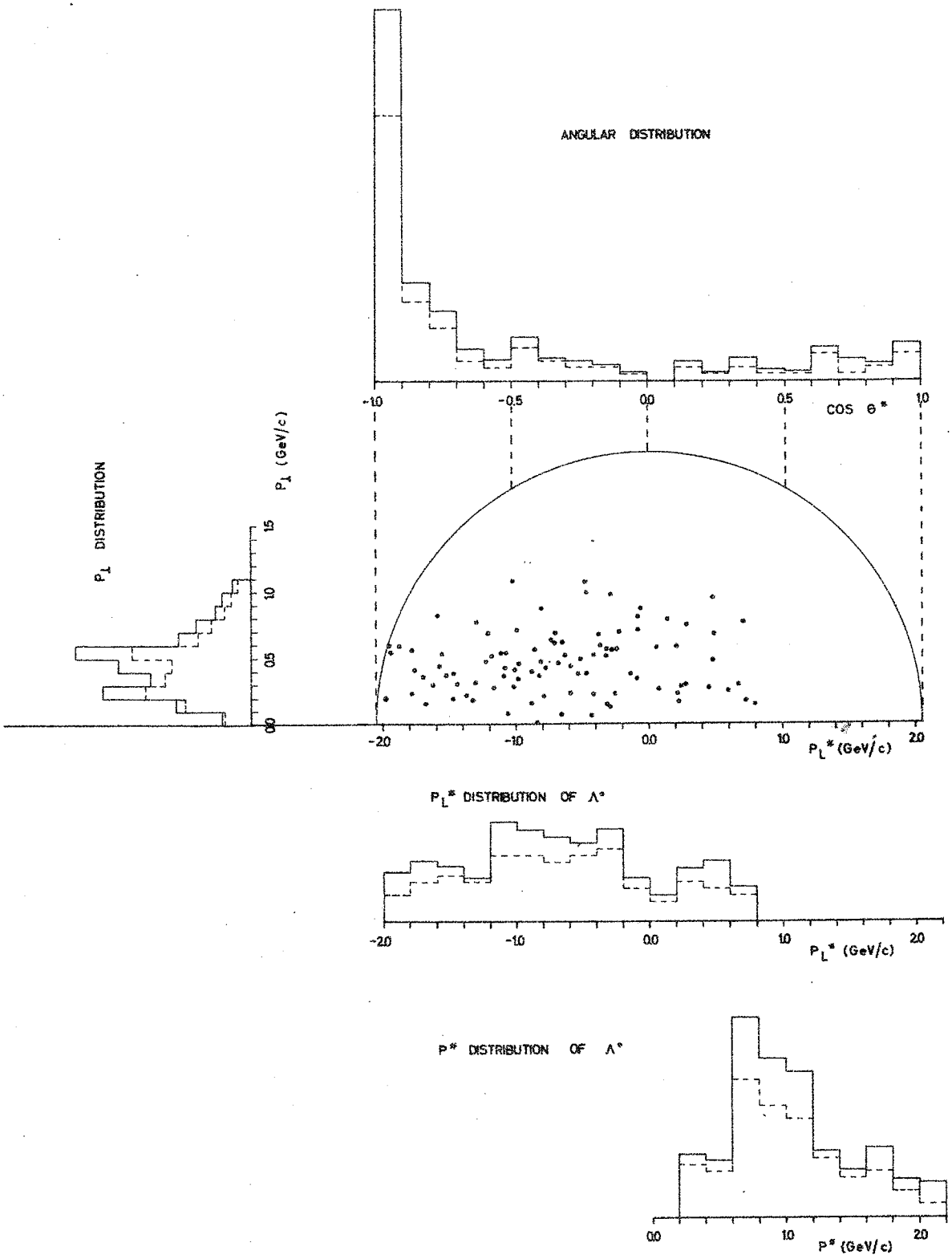

Fig. 1

DIA - 18637
PS/4195

$K^{\circ}\Lambda^{\circ}$ PRODUCTION

$P_T P_L^*$ PLOT FOR K°

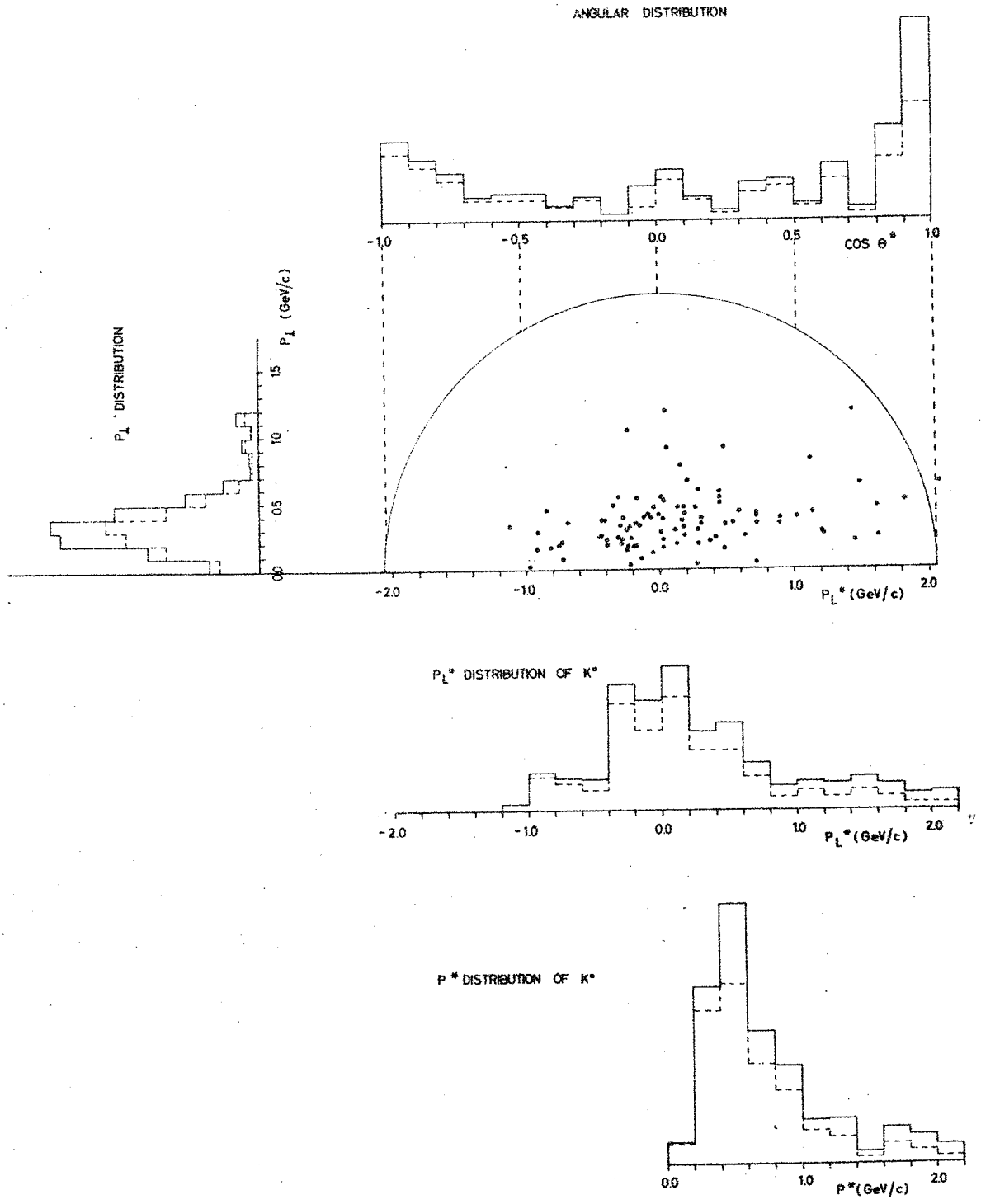

Fig. 2

DIA · 19517
PS/4195

$K^{\circ}\Lambda^{\circ}$ PRODUCTION

$P_{\perp}$-P_{L}^{*} PLOT FOR $\pi^{\pm}$

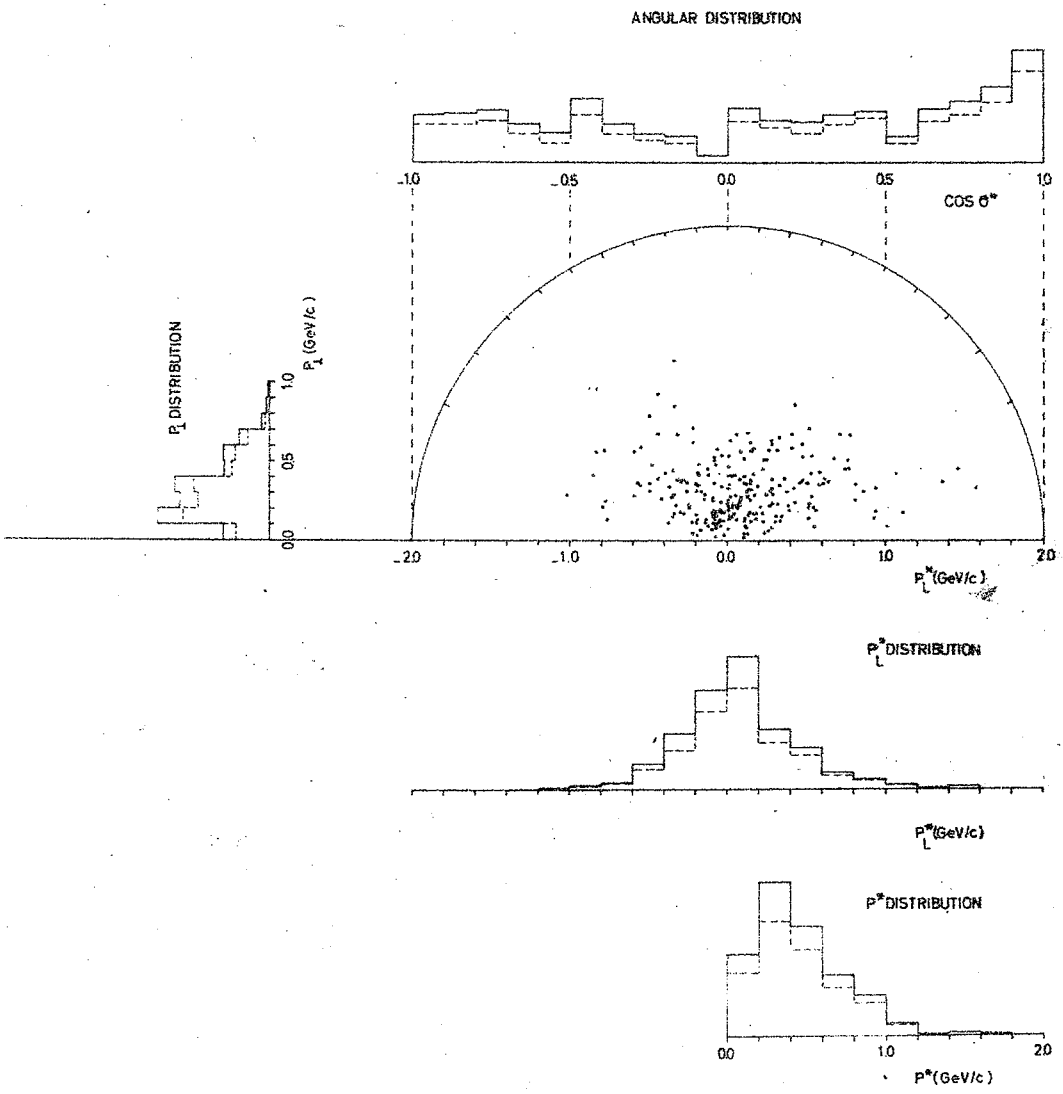

Fig.3

DIA - 19406
PS/4195

P_T-P_L^* PLOT FOR Σ^+ PRODUCTION

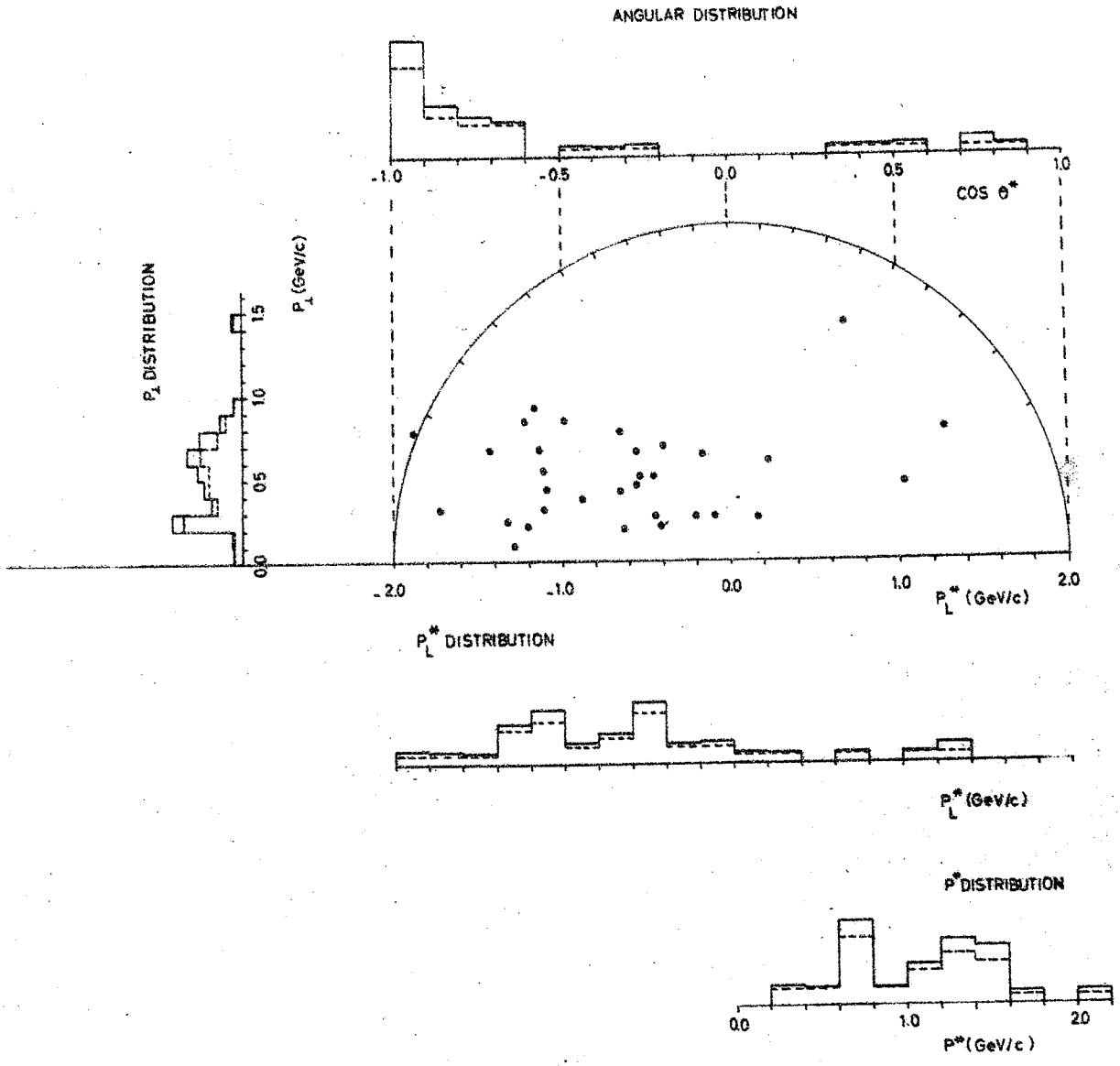

Fig. 4

DIA - 18867
PS/4195

$P_\perp - P_L^*$ PLOT FOR K° PRODUCED WITH Σ^+

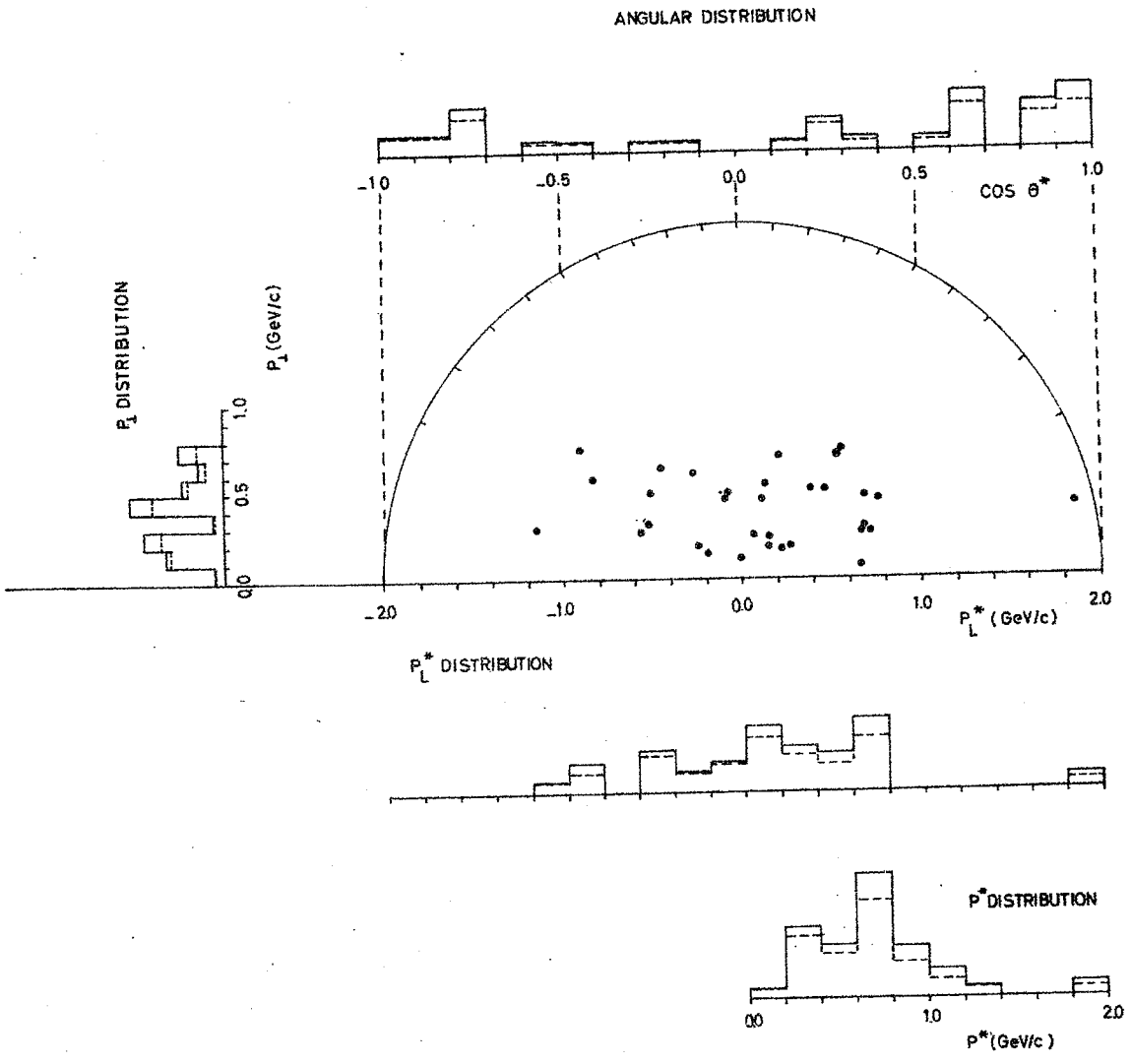

Fig. 5

DIA - 19520
PS/4195

$K^{\circ}\Sigma^{+}$ PRODUCTION

$P_{\perp}$-P_L^* PLOT FOR $\pi^{\pm}$.

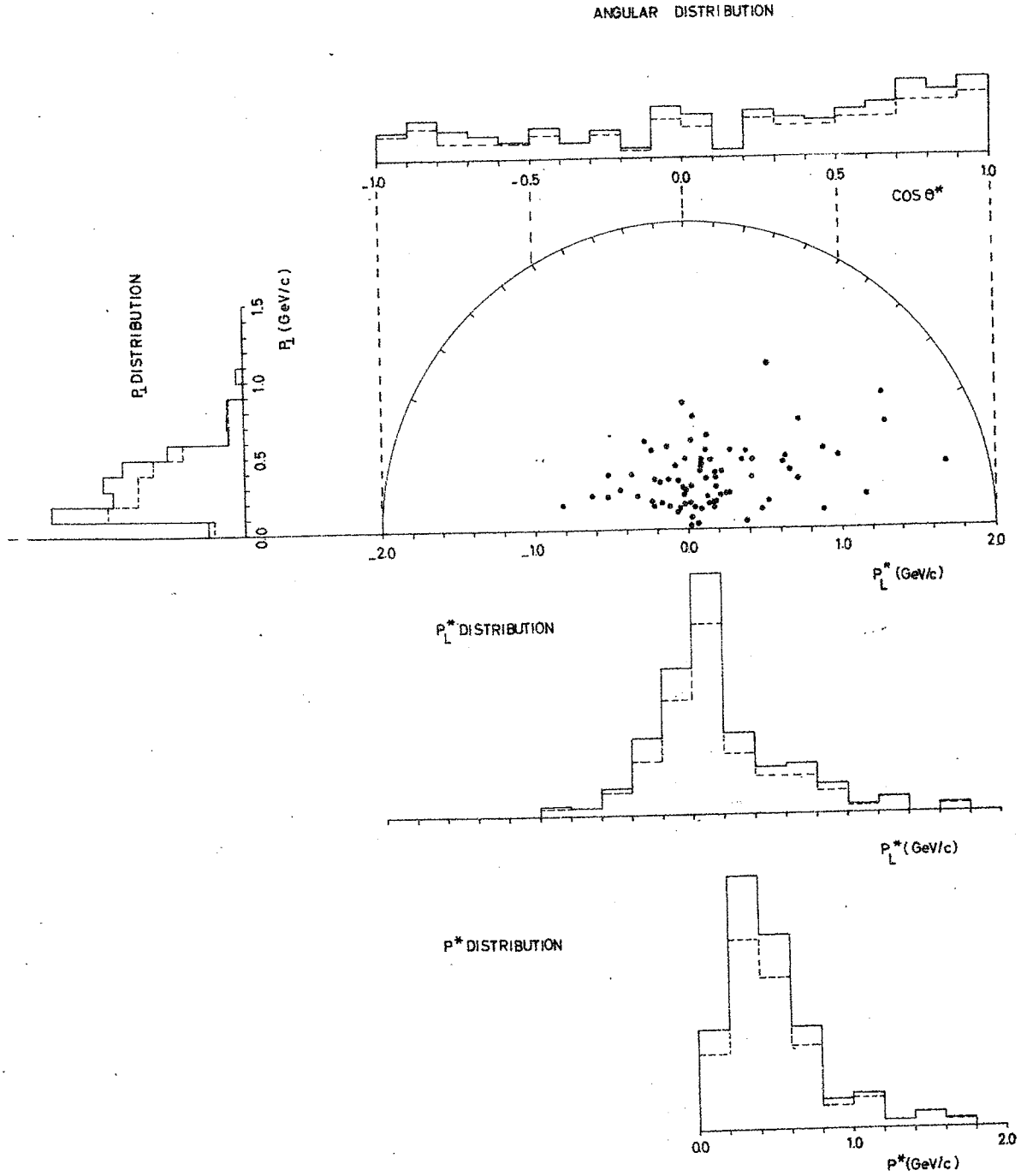

Fig .6

DIA-19404
PS/4195

$P_\perp - P_L^*$ PLOT FOR Σ^- PRODUCTION

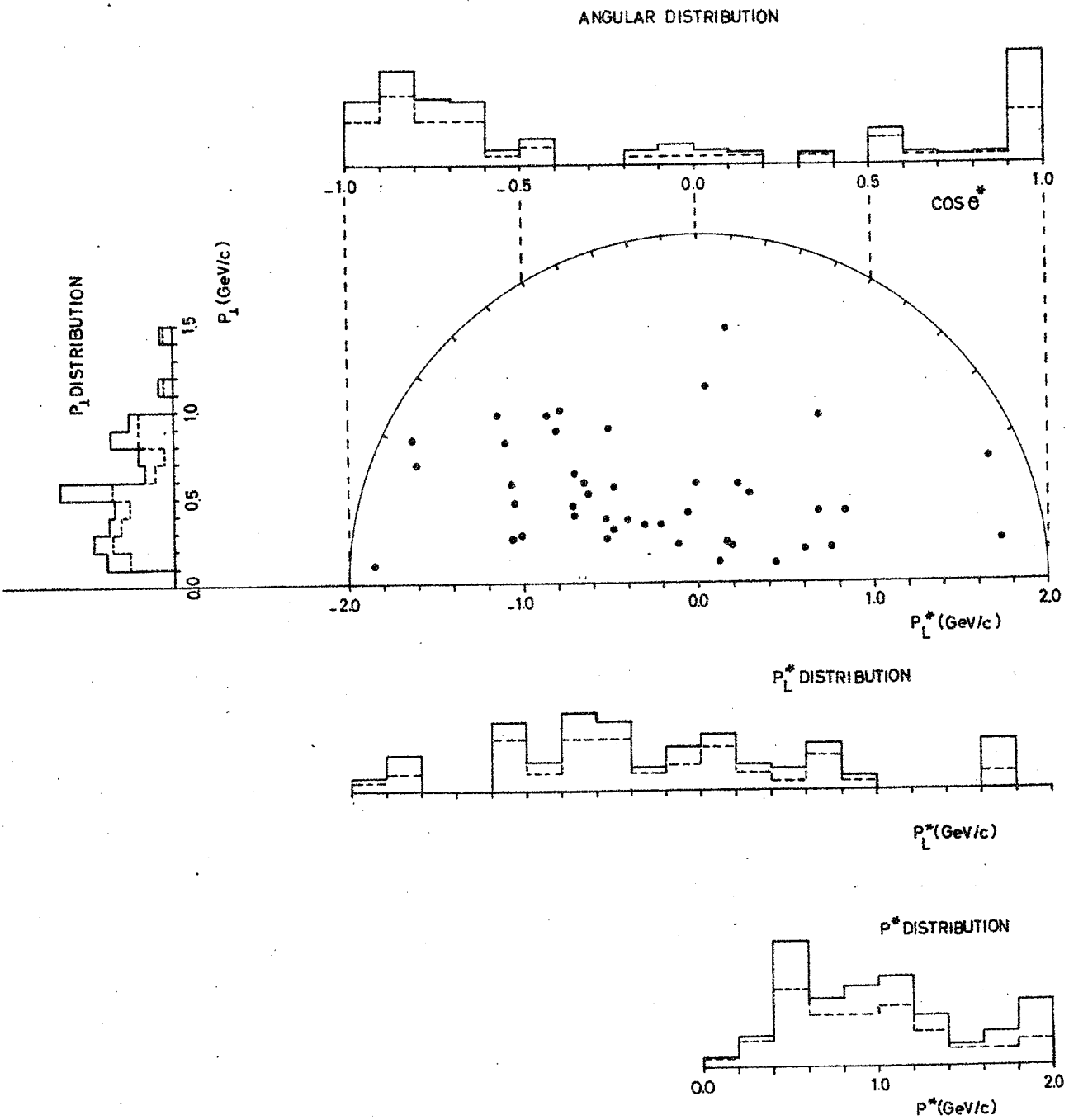

Fig.7

DIA - 18868
PS/4195

$P_\perp - P_L^*$ PLOT FOR K° PRODUCED WITH Σ^-

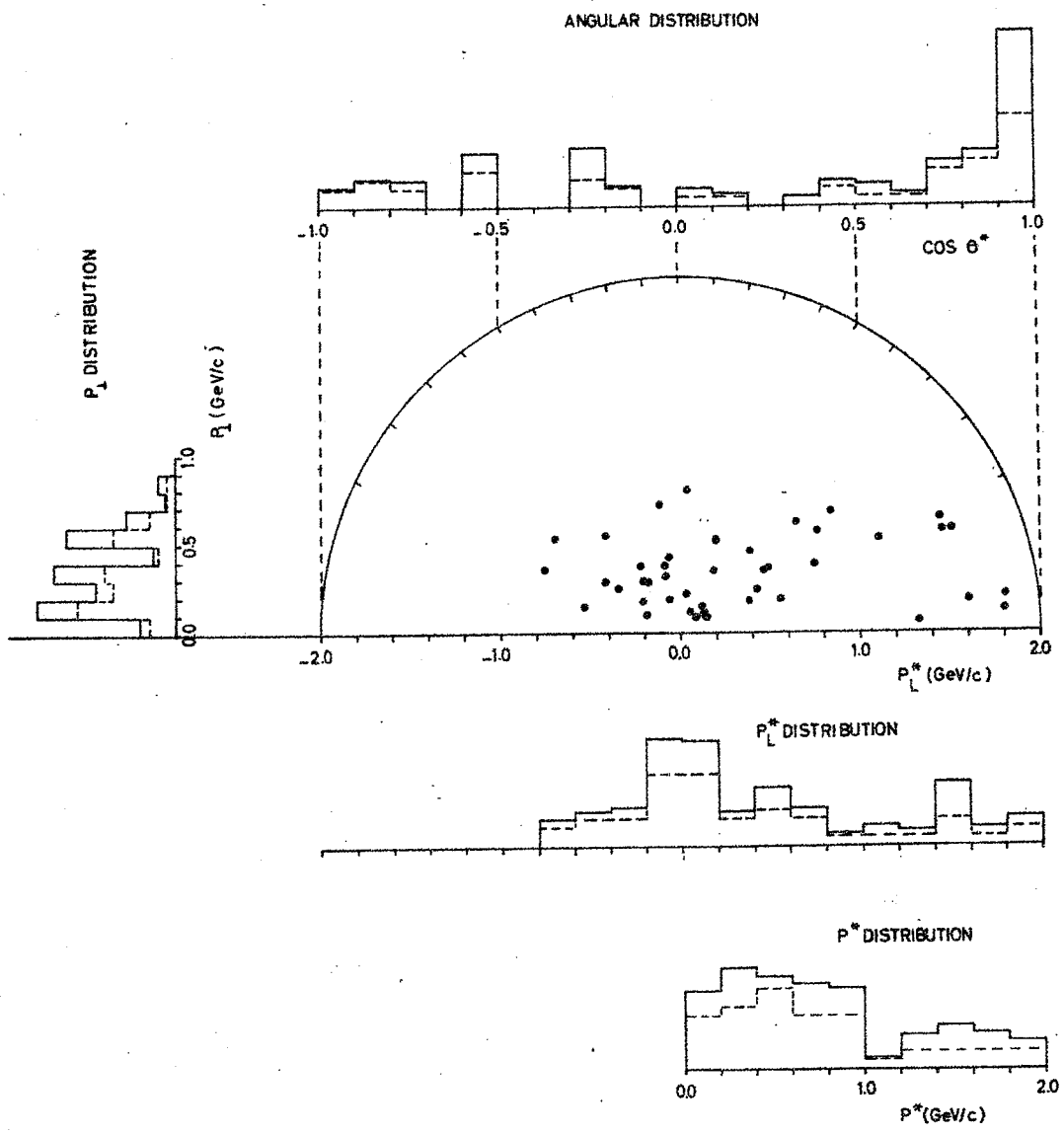

Fig.8

DIA - 19522
PS/4195

$K^{\circ}\Sigma^{-}$ PRODUCTION

$P_{\perp}$-P_L^* PLOT FOR $\pi^{\pm}$

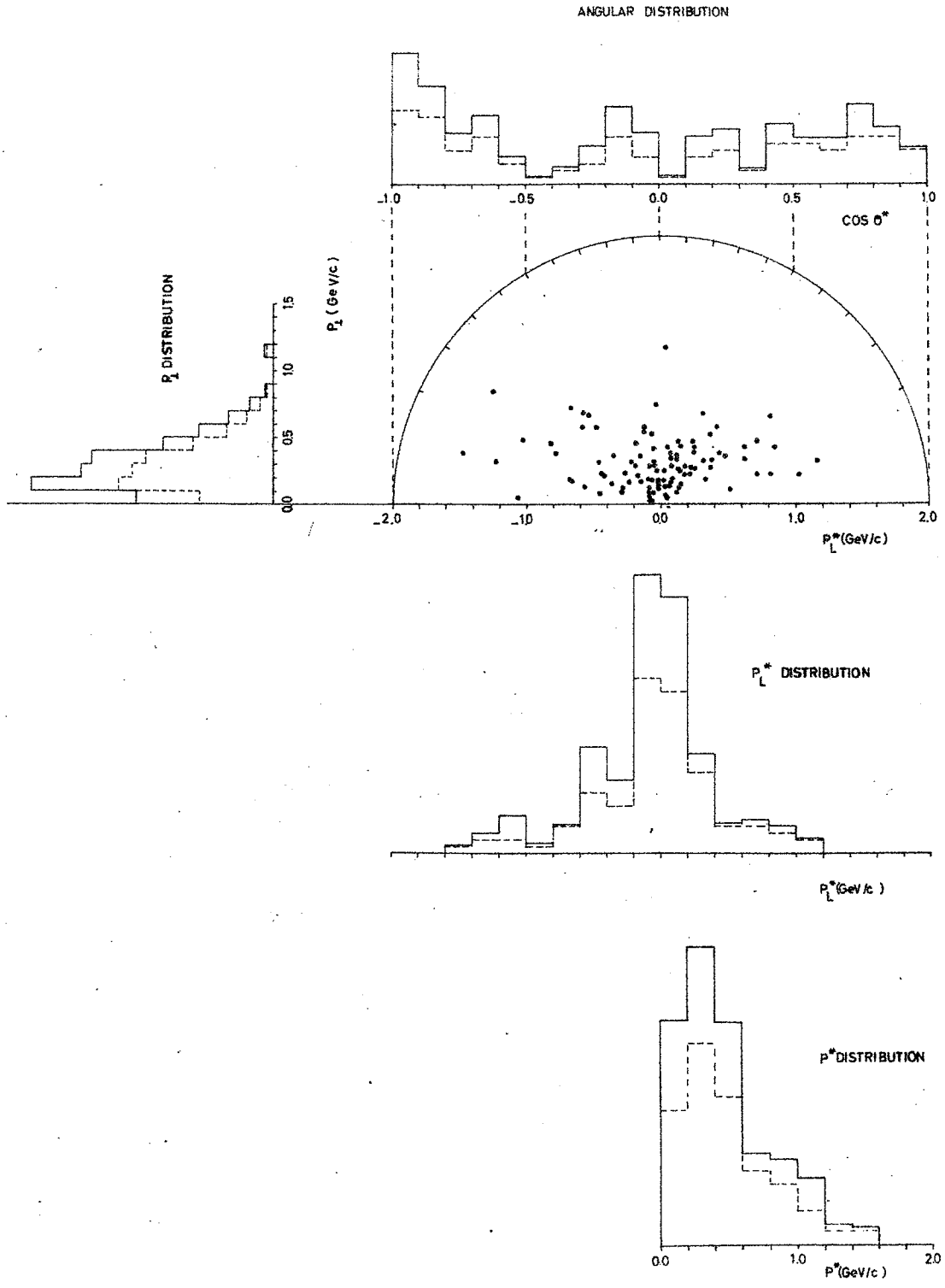

Fig.9

DIA - 19407
PS/4195

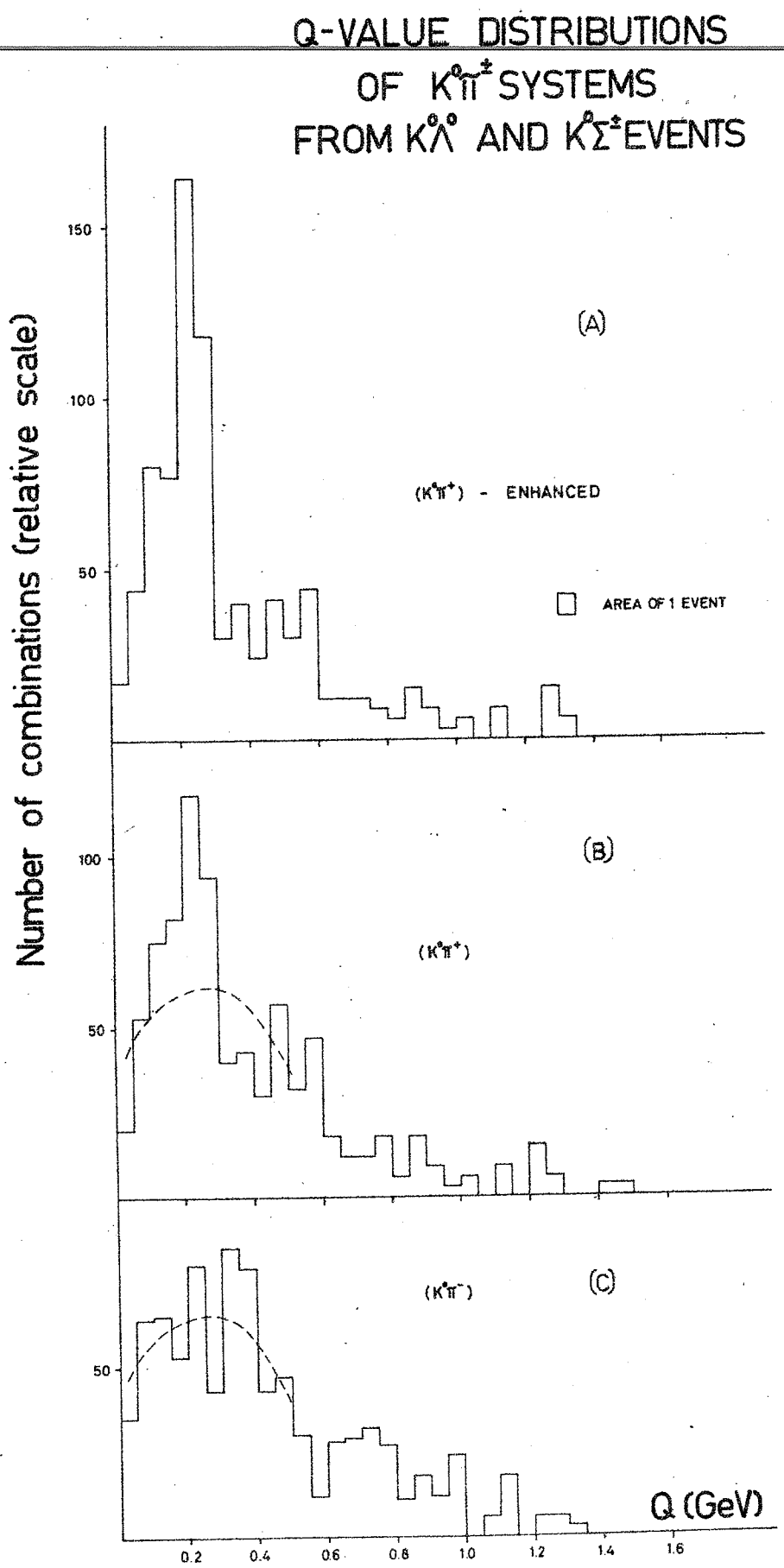

Fig .10

DIA - 19411
PS/4195

DIA - 18405
PS/4795

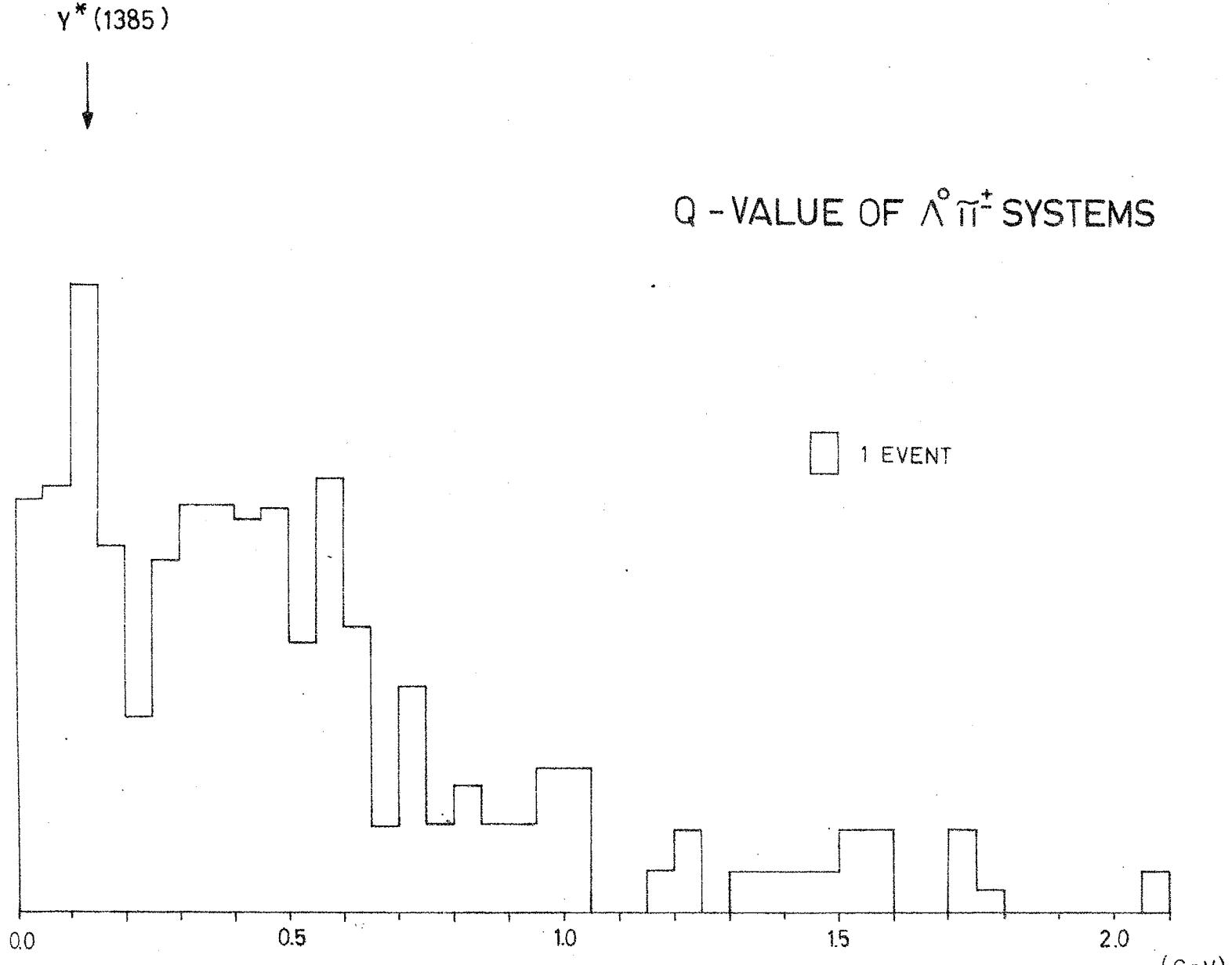

Fig . 11

DIA - 19408
PS/4475

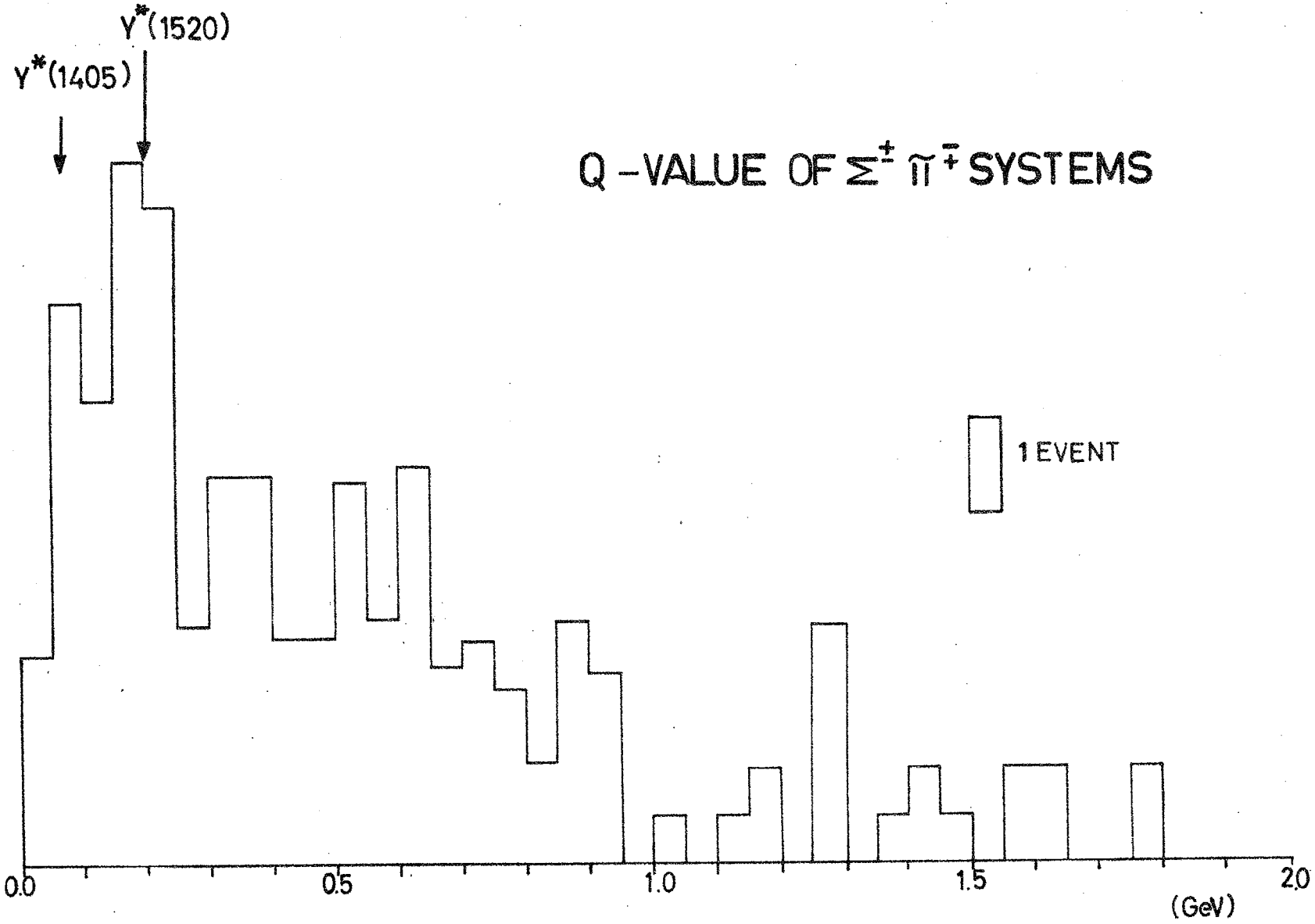

Fig. 12

$P_\perp$ DISTRIBUTIONS

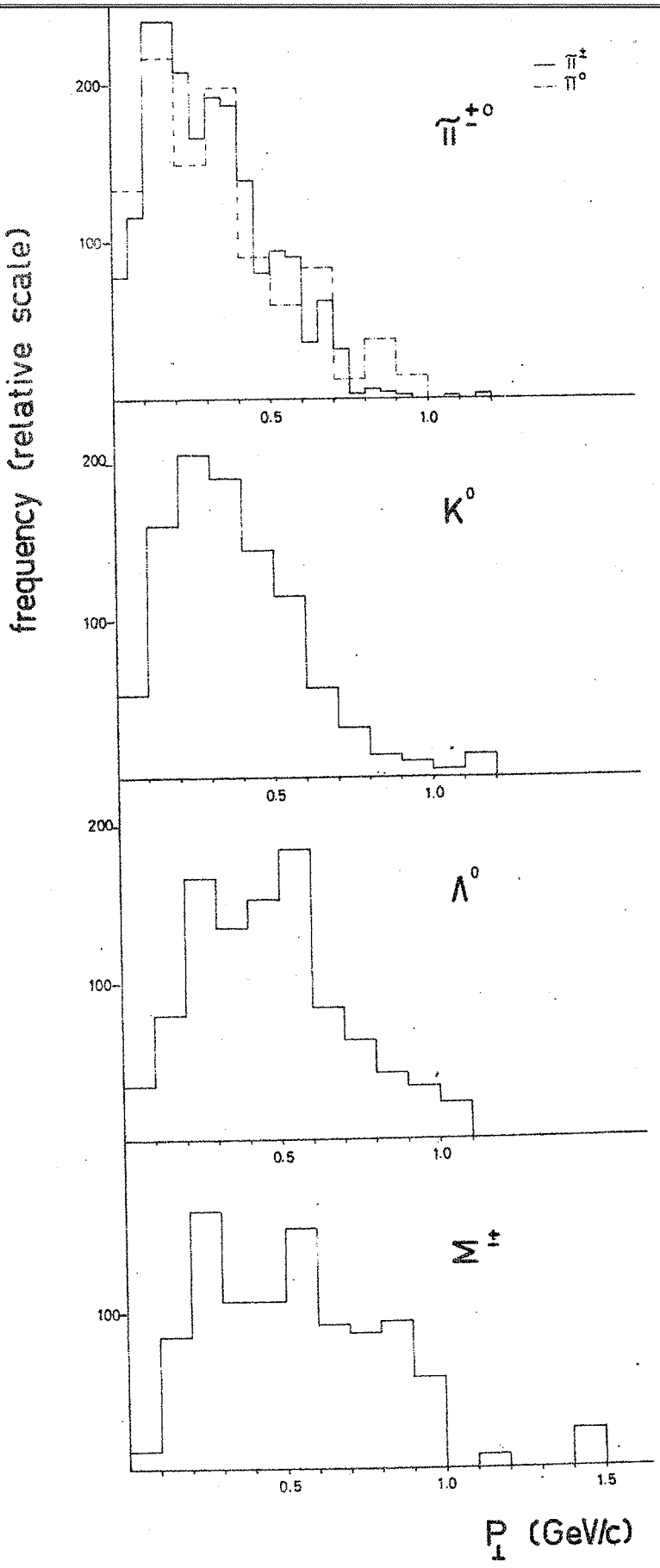

Fig.13

DIA - 19413
PS/4 195

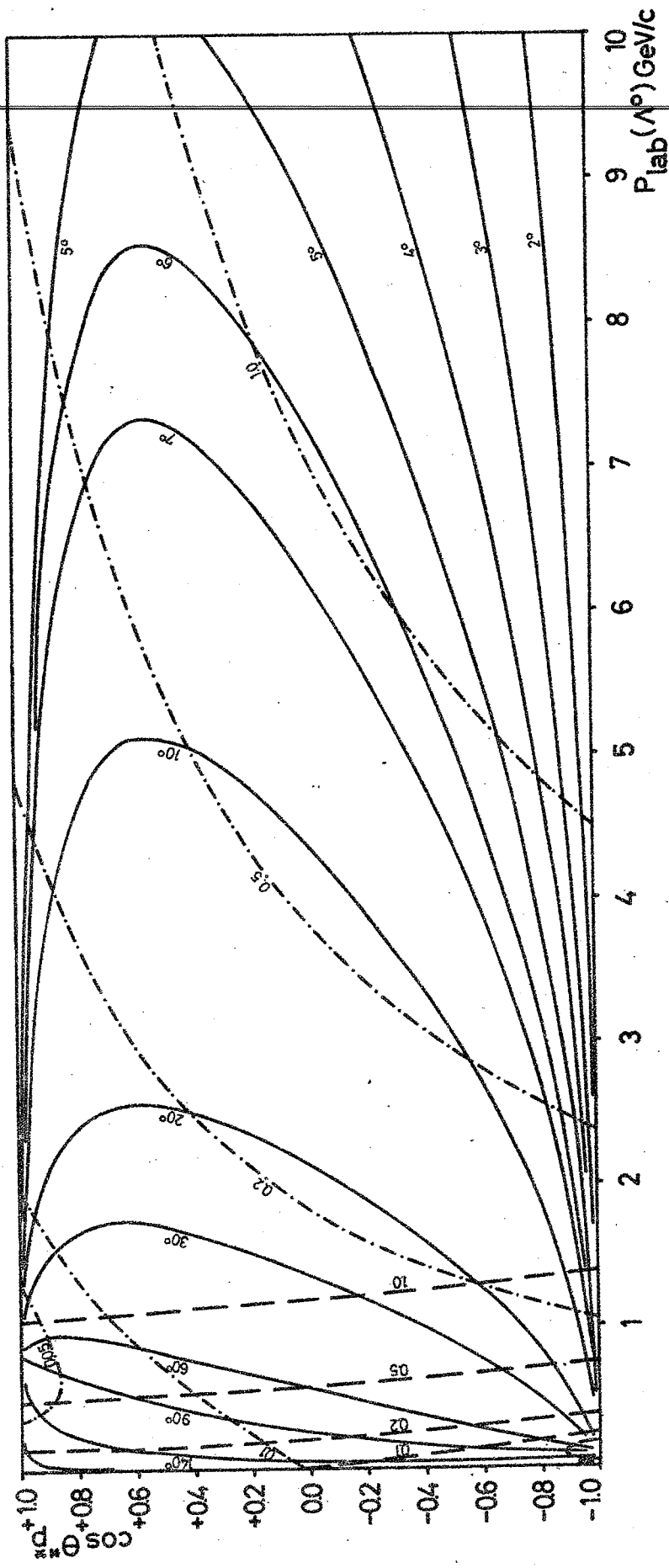

Fig. 14

DIA - 19518
PS/4195

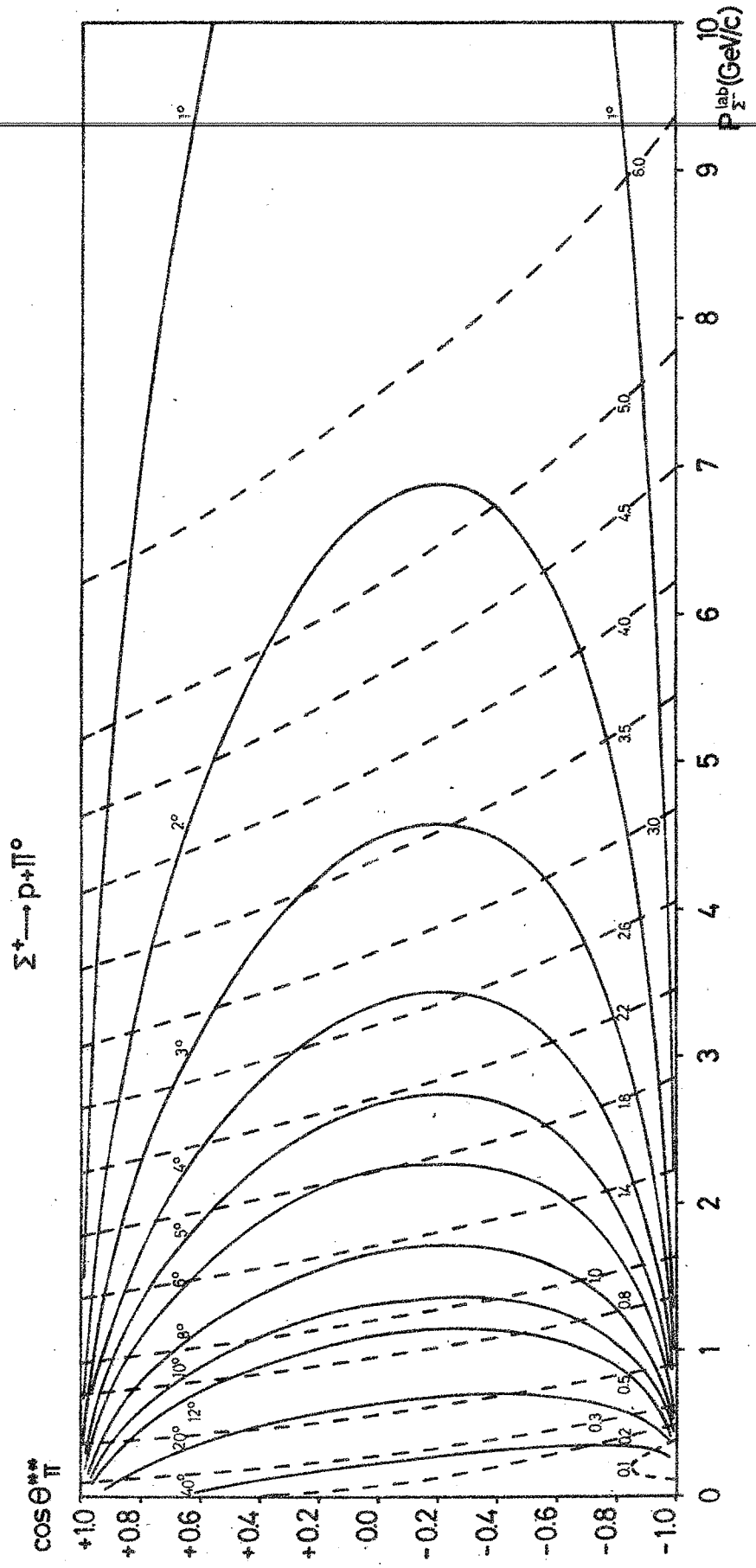

Fig. 15

DIA - 19531
PS/4195

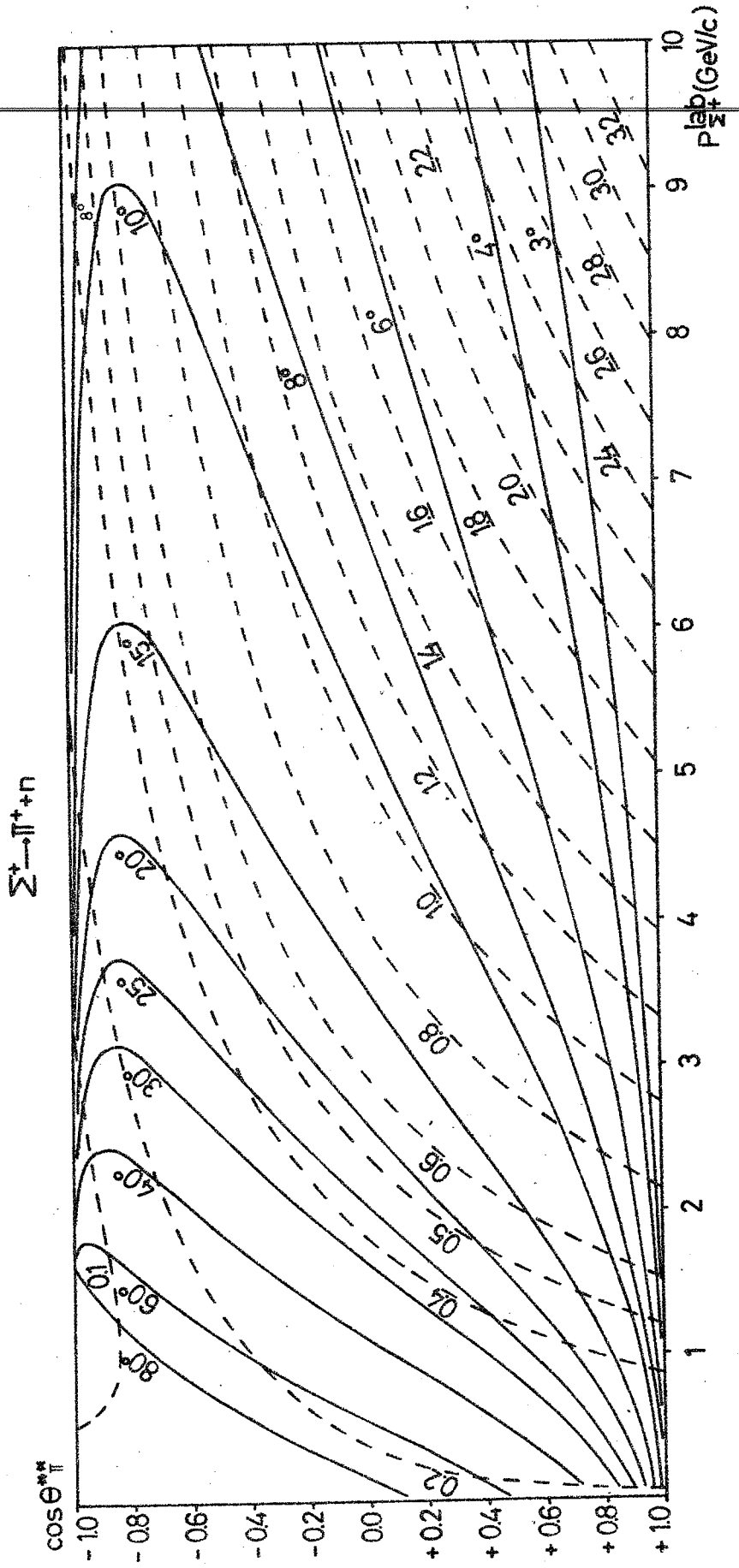

Fig. 16

DIA - 19519
PS/4195

DIA - 19409
PS/4195

EFFICIENCY OF TWO SCANNINGS

VS. ANGLE OF $V^{\pm}$

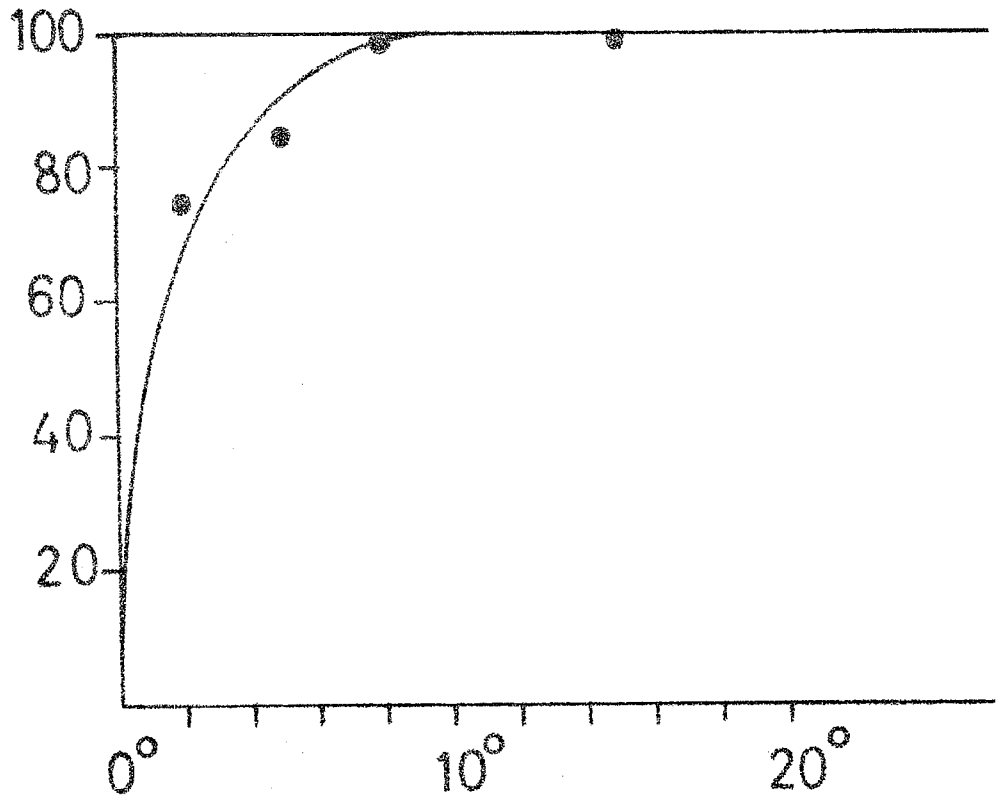

Fig. 17

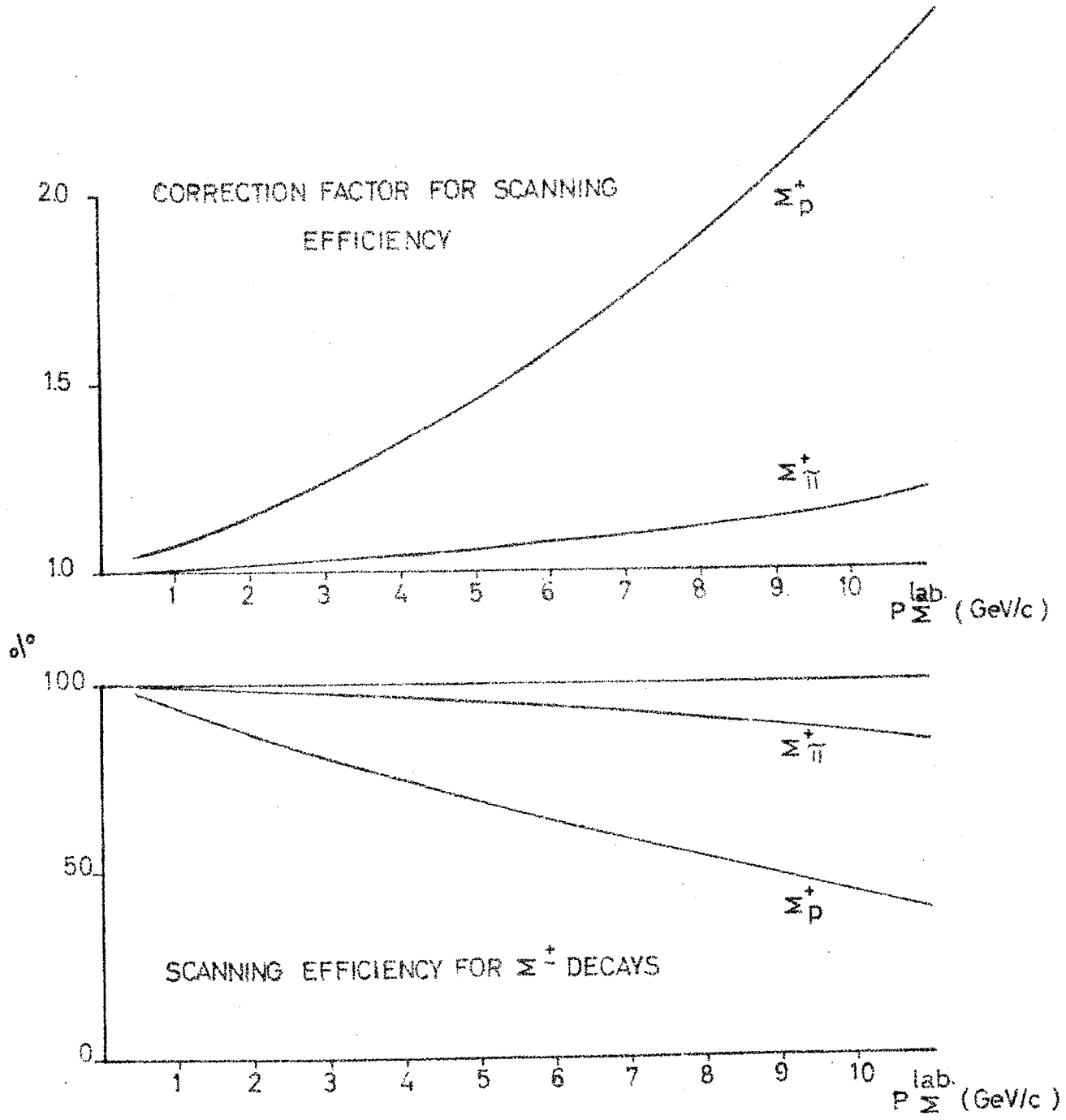

Fig. 18

DIA - 19516
PS/4195